Online ISSN 1848-3380, Print ISSN 0005-1144
ATKAFF 53(3), 244–254(2012)

Mario Jurković, Damir Žarko

Optimized Design of a Brushless DC Permanent Magnet Motor for Propulsion of an Ultra Light Aircraft

DOI 10.7305/automatika.53-3.114
UDK 621.313.8.047.2:629.73
IFAC 2.1.4; 4.7.0

Original scientific paper

The paper presents an optimized design of a low mass brushless DC (BLDC) permanent magnet motor for propulsion of an ultra light aircraft. The optimization has been carried out using Differential Evolution algorithm implemented in Matlab combined with SPEED and MotorCAD software packages for electromagnetic and thermal modeling of the BLDC motor using ActiveX technology. The credibility of the models created with SPEED and MotorCAD has been confirmed by comparing the results of simulation and measurement performed on a 12 kW synchronous permanent magnet motor available in the laboratory. The goal of the optimization has been to minimize the weight of the motor under condition that the motor delivers rated power of 15 kW at rated speed of 3000 rpm with hot-spot temperature not exceeding the temperature limits of class F insulation (155 °C). Two optimal BLDC motor designs with slot/pole combinations 12/10 and 18/16 have been obtained. The motor with 18 slots and 16 poles yields the highest torque density with the lowest mass of active parts (copper+laminations+magnets) of only 5.1 kg.

Key words: Aircraft, Brushless DC motor, Permanent magnet motor, Optimization, Differential evolution

Optimirani projekt elektronički komutiranog motora s trajnim magnetima za pogon ultra lake letjelice. U članku je prikazan optimirani projekt elektronički komutiranog motora (EKM) s trajnim magnetima male mase za pogon ultra lake letjelice. Optimizacija je provedena korištenjem algoritma pod nazivom Diferencijalna evolucija koji je primijenjen u Matlabu u kombinaciji s programskim paketima SPEED i MotorCAD za elektromagnetski i termički proračun EKM-a koristeći ActiveX tehnologiju. Vjerodostojnost modela načinjenih u SPEED-u i MotorCAD-u je potvrđena usporedbom rezultata simulacije i mjerenja obavljenih na sinkronom motoru s trajnim magnetima koji je bio na raspolaganju u laboratoriju. Cilj optimizacije je bio minimizirati masu motora pod uvjetom da motor razvija nazivnu snagu 15 kW pri nazivnoj brzini vrtnje 3000 min^{-1} pri čemu temperatura najtoplije točke namota ne smije prijeći granicu određenu klasom izolacije F (155 °C). Načinjena su dva optimalna projekta EKM-a s kombinacijama broja utora i polova 12/10 i 18/16. Motor s 18 utora i 16 polova postiže najveću gustoću momenta uz najmanju masu aktivnih dijelova (bakar+jezgra+magneti) koja iznosi samo 5,1 kg.

Ključne riječi: letjelica, elektronički komutirani motor, motor s trajnim magnetima, optimizacija, diferencijalna evolucija

1 INTRODUCTION

Each glider pilot would appreciate that, in the case of altitude loss, he or she can turn the motor on and fly away to a different location to search for rising air currents. From this practical need an idea for a glider motor was born. An electric motor is ideal for this purpose because it is reliable and easy to handle, it does not need maintenance and needs less instruments for monitoring its condition than in the case of internal combustion engines. The only drawback of the electric motor is power supply which is typically the heaviest part of the glider electrical system.

A permanent magnet (PM) motor is the most suitable type of motor for this application due its lower mass, higher efficiency and higher torque density compared to an induction motor or a DC motor. When comparing various types of PM motors, the BLDC motor emerges as a suitable candidate due to higher torque density than synchronous PM motors [1]. An example of design optimization of a BLDC motor for a solar airplane has been presented in [2]. A fairly simple analytical electromagnetic and thermal models have been used together with ProDesign software which utilizes Sequential Quadratic Programming for optimization. The mass was chosen as the objective function. To avoid additional weight, the motor was designed without its own housing. The choice between standard or straight tooth shape has been made manually according to

the results presented in [3] which indicate that the straight tooth design yields lower mass of the motor. The final result of the optimization process based on which a prototype has been built is presented in [4]. The rated mechanical power is 12 kW, the rated speed is 530 rpm and the total mass is 37 kg. The results of measurements performed on the prototype show that the actual efficiency at 8.3 kW of mechanical power and the speed of 470 rpm is 92.1 % instead of 96.5 % as predicted analytically.

In [5] a multi-disc axial flux permanent magnet motor rated 1.25 kW for propulsion of a stratospheric unmanned aircraft has been analyzed. It has been shown that the axial flux design with the airgap concentrated second harmonic windings has a 10 % lower mass than a radial flux machine. However, its main disadvantage is almost seven times more weight of permanent magnets required for the same power output because it utilizes an air-gap winding.

Another option under investigation for aircraft propulsion are high temperature superconducting (HTS) motors due to their high power density. Masson et al. [6] analyzed a HTS motor for Cessna 172SP aircraft. The results indicate that a total system (HTS motor+cryocooler) would weigh about 100 kg while the conventional internal combustion engine for this aircraft rated 120–135 kW weighs about 160 kg. A slightly different design of a HTS motor for Cessna 172SP optimized in terms of power density is presented in [7]. In [8] the scaling up of this design to 1.5 MW for the purpose of replacing turbofan gas turbines by electrical motors in an aircraft is shown. A case study of a 450 kW HTS axial flux configuration has also been made [9]. This design allows stacking up of several rotors and stators and therefore enables the use of one or several conventional permanent magnet rotors to generate minimum safety torque in case of loss of superconductivity. The main issue of HTS technology in all these cases is high cost.

This paper describes design optimization of a BLDC motor for an ultralight aircraft using Differential evolution (DE) optimization algorithm implemented in Matlab-SPEED-MotorCAD system where SPEED has been used for electromagnetic calculation and MotorCAD for thermal calculation. The motor configuration with fractional slot concentrated winding has been selected due to high power density, high efficiency, short end turns and high slot fill factor [10]. The tooth shape has been fully determined by the optimization process. The volume of the active part has been chosen as the objective function. The result of the optimization process is a BLDC motor rated 15 kW, 3000 rpm which weighs 5.1 kg (total mass of iron, copper and magnets excluding shaft and housing). The total mass including shaft and housing is around 8 kg.

2 MODEL EVALUATION USING AN SPM MOTOR

The brushless DC motor for an ultra light aircraft presented in this paper is a design study at this stage, so there is no prototype available for experimental evaluation of the design. However, in order to ensure a reliable correlation between the designed and the actual performance, the design software SPEED and MotorCAD have been evaluated by modeling a synchronous permanent magnet motor (SPM) rated 12 kW, 1800 rpm available in the laboratory at the University of Zagreb, Faculty of Electrical Engineering and Computing. This motor has a geometry similar to the geometry of the BLDC motor. The results of tests performed on the SPM motor have been used to confirm the credibility of the electromagnetic and thermal models used for the BLDC motor design.

2.1 Armature winding resistance

The armature winding resistance has been determined by measuring the current and the voltage drop across each individual winding powered from a DC source. The mean value of the measured armature winding resistance for all phases was 135,7 mΩ and the ambient temperature was 21 °C. This motor has an overlapping short-pitched double-layer winding.

The measurement results have been used to adjust the wire length in the end winding in order to obtain the correct value of the armature winding resistance parameter in SPEED. That is necessary to obtain more accurate power and loss calculation.

2.2 Electromagnetic model in SPEED

The PC-BDC program, which is a part of the SPEED software, has been used to model the SPM motor and to design the BLDC motors. The PC-BDC is intended for analytical modeling of synchronous and brushless DC permanent-magnet motors, drives, line-start PM motors and wound-field synchronous machines. The design with PC-BDC is interactive and fast. However, the PC-BDC does not produce an optimized design by itself. In our case it is used as a tool for calculating the parameters and the performance of the motor in a repetitive iterative optimization scheme in which numerous motor designs are created, simulated and compared to other designs until the desired objectives are achieved, i.e. the minimum value of the objective function is found.

In the first step the user must enter parameters of the materials used for motor construction. That is done in the SPUD environment in SPEED. After that the user starts the PC-BDC program and generates an initial model using the Outline editor. After generating the initial model the geometric, electrical, magnetic and winding parameters are entered. The Outline editor is shown in Fig. 1. After entering all the parameters it is necessary to run the dynamic analysis to complete the electromagnetic simulation.

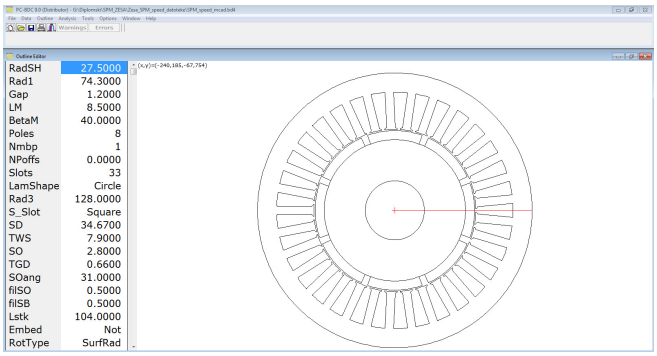

Fig. 1. Outline editor in SPEED, radial view

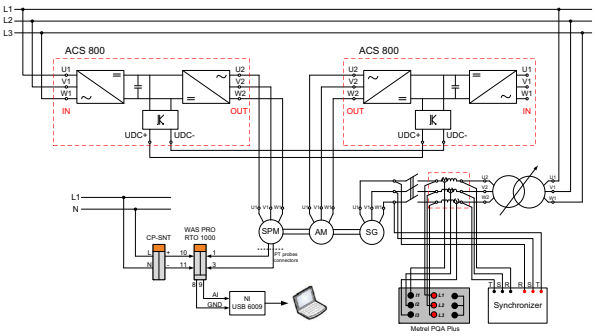

Fig. 2. Measurement scheme for the load test

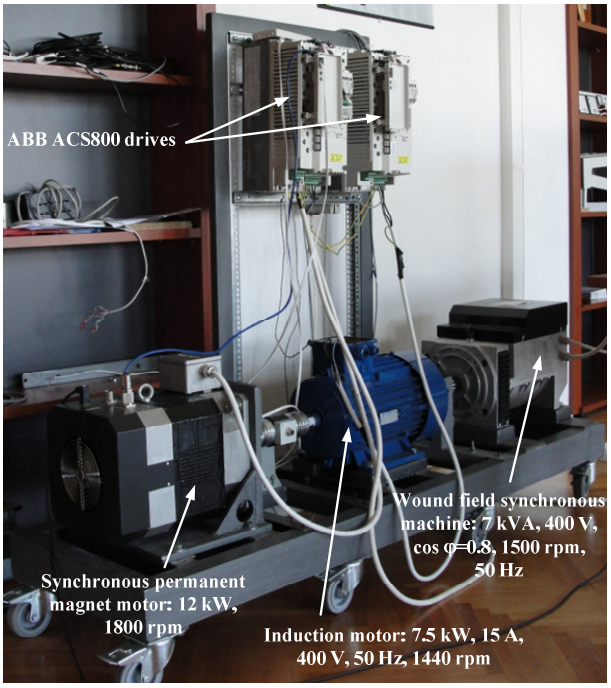

Fig. 3. Hardware setup for the load test

2.3 Thermal model in MotorCAD

After running the PC-BDC program and obtaining the results of the dynamic simulation, the SPEED model is imported into MotorCAD and the thermal model is created. The user must enter a few additional parameters that are not imported from SPEED. Those parameters are related to cooling type, the size of the frame and the cooling fins, and the air speed along the motor frame. The air speed is measured using anemometer since the motor has a fan mounted of the rear side which blows the cooling air along the frame.

2.4 Load test

The purpose of the load test is to determine the time variation of the winding temperature at rated load and compare it to the results of the dynamic thermal simulation in MotorCAD. The SPM motor is loaded simultaneously with an induction and a synchronous machine mounted on the same shaft and both operating in the generating mode. The induction machine is powered from an ABB ACS800 AC drive which shares a common DC bus with the AC drive to which the SPM motor is connected. The synchronous machine is synchronized to the power grid at 1500 rpm and its torque is regulated by adjusting the torque of the SPM machine running in the DTC mode. The induction machine also runs in the DTC mode with the torque reference equal to its rated torque. The winding temperatures of the SPM motor are measured using PT1000 temperature probes. The probes are connected to operational amplifiers WAS PRO RTO 1000, which pass the voltage signal to the DAQ card (acquisition system). The DAQ card performs A/D conversion and sends the data to the computer. The computer data is processed in the software package LabVIEW 2010. The measurement scheme for the load test is shown in Fig. 2, and the hardware setup with the machine ratings is shown in Fig. 3.

The results of the load test and simulation in MotorCAD are compared in Fig. 4. The temperature of the probe fitted in the winding where the measured temperature is the highest has been displayed. For the armature current 20 A the maximum measured temperature is 80 °C and the maximum temperature from MotorCAD static calculation is 80.6 °C (the ambient temperature is 19 °C). For the current 24 A (not shown in Fig. 4) the maximum measured temperature is 90 °C and the maximum temperature from MotorCAD static calculation is 92.4 °C.

There is a very good match between measured and calculated temperature at steady state. However, there is a difference between temperatures obtained during the thermal transient. For thermal transient simulations it is necessary to have correct values of thermal resistances and thermal capacitances. It appears that the values of thermal capacitances should be corrected for more accurate calculation

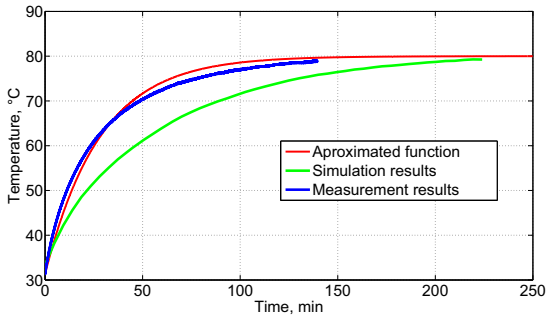

Fig. 4. The results of load test and simulation in Motor-CAD

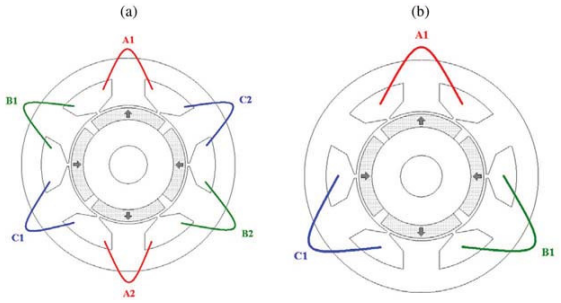

Fig. 5. Concentrated stator winding configuration: (a) All teeth wound, (b) Alternate teeth wound [10].

of the temperature. In our case the default values given by MotorCAD have been used. Nevertheless, based on this example it appears that the steady state temperature can be calculated reliably using the default MotorCAD thermal model. This is essential from the aspect of the motor design, since for this particular application in the ultra light aircraft the steady state operation of the motor is primarily considered.

3 BLDC MOTOR

After validation of results from electromagnetic and thermal models of the SPM motor, one can approach the design of the BLDC motor for the ultra light aircraft. Two models of the BLDC motor have been designed. The first model is with 12 slots and 10 poles and the second is with 18 slots and 16 poles. After finding the optimal solution for the first model, the goal was to increase the number of poles and slots in the second model with an attempt to yield further reduction in mass and volume. The BLDC motor with larger number of poles has a higher torque density per volume and the increase in the number of poles resulted in a reduction of diameter and the axial length of the motor, and thus the mass and volume.

3.1 Winding configuration

The nonoverlapping, i.e. concentrated winding configuration is most commonly used for BLDC motors. The concentrated winding can have either all teeth or alternate teeth wound (Fig. 5). [11]

The winding with alternate teeth wound has a more trapezoidal back-EMF waveform, but MotorCAD does not recognize that winding configuration. Therefore, the winding with all teeth wound has been used. After selecting the winding configuration it is necessary to choose the number of slots and poles according to the formula [11]

$$2p = N_s \pm 2. \tag{1}$$

where p is the number of pole pairs and N_s is the number of slots. Thus, the typical $N_s/2p$ combinations are 6/4, 6/8; 12/10, 12/14; 18/16, 18/20; 24/22, 24/26; ..., etc. The merits of such combinations include the following:

- slot-pitch almost equal to the pole-pitch, which is conducive to a high coil flux-linkage and torque density;
- fractional ratio of slot number to pole number, which is conducive to a low cogging torque.

All teeth wound winding configurations for different slot/pole combinations are shown in Table 1 and Fig. 6.

Table 1. All teeth wound winding configuration for different slot/pole combinations [11]

Slots/poles	Winding configuration
12/10	AA'B'BCC'A'ABB'C'C
18/16	A'AA'B'BB'C'CC'A'AA'B'BB'C'CC'

3.2 Initial model

Before the start of optimization the user must create an initial model in SPEED by entering the starting geometry and defining all the parameters in accordance with the purpose and type of the motor. The purpose of this model is to set all the parameters required for running the SPEED model which will remain constant during the optimization process. For instance, those parameters are used to define slot type, winding connection, drive type, DC bus voltage or to define various calculation methods for back EMF, torque, phase terminal voltage, iron or magnet losses etc. During the optimization process this initial model is always used to transfer the geometric data of the current design produced by the DE algorithm from Matlab to SPEED, run the simulation and return the results to Matlab to calculate the constraint functions and the cost function

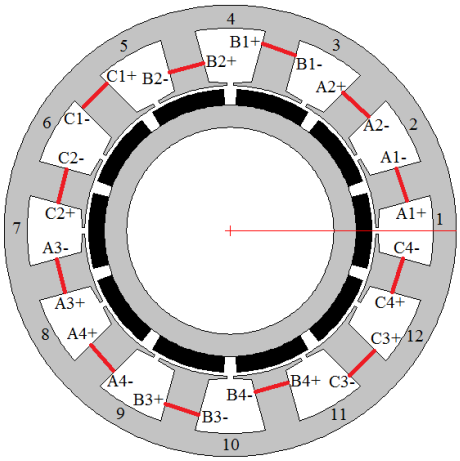

(a) 12/10

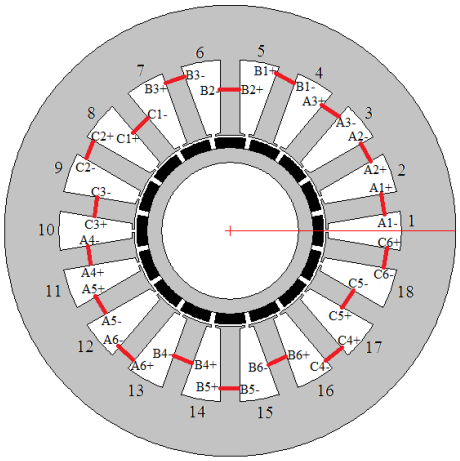

(b) 18/16

Fig. 6. All teeth wound winding configuration for different slot/pole combinations

for the DE. The initial model itself does not need to satisfy any constraints of the optimization. It is only important that the dynamic simulation can be performed without errors. The initial model parameters and constraints of optimization should be well defined so that the user does not have to manually intervene in case of failure.

The design with 12 slots and 10 poles according to [11] has been selected for the initial model. Table 2 shows the list of parameters of the initial model. The motor in [11] is rated 36 V (DC bus voltage), 400 rpm and 5.5 Nm. In our case the selected values are 100 V, 3000 rpm and 47.5 Nm because of specific requirements for applications in aviation.

All parameters, which are not optimized, remain the same as defined in the initial model. The parameter $BetaM$, which is the pole arc (magnet width defined in deegres), is calculated according to [12].

Table 2. List of parameters of the initial model for the BLDC motor [11]

Parameter	Value
Supply DC bus voltage (V_{DC}), V	100
Rated torque (T_r), Nm	47.5
Rated speed (n_r), rpm	3000
Number of slots (Q_S)	12
Number of poles ($2p$)	10
Stator outer radius ($D_o/2$), mm	50
Stator inner radius ($D/2$), mm	28.5
Tooth thickness (TWS), mm	7.1
Slot opening (SO), mm	2
Slot depth (SD), mm	17.8
Thickness of the stator tooth tip (TGD), mm	2.6
Stack length (L_{stk}), mm	50
Airgap length (δ), mm	1
Shaft radius ($RadSH$), mm	16
Magnet thickness (h_m), mm	3

The smallest common multiple between the number of slots and the number of poles for the 12/10 model is $N_c = 60$, so the optimal magnet pole-arc is

$$\alpha_p = \frac{\frac{N_c}{2p} - k_1}{\frac{N_c}{2p}} + k_2 = \frac{6-1}{6} + 0.02 = 0.8533$$

where α_p is the optimum ratio of the pole arc to pole pitch, $k_1 = 1, 2, ..., \frac{N_c}{2p}$ and k_2 is the fringing coefficient typically ranging from 0.01 to 0.03. The value of k_1 is set to 1 to yield the widest magnet pole arc. The magnet pole arc in electrical degrees is then

$$\Rightarrow BetaM = 0.8533 \cdot 180°\text{el} = 153.6°\text{el}. \qquad (2)$$

The smallest common multiple between the number of slots and the number of poles for the 18/16 model is $N_c = 144$, so the optimal magnet pole arc is

$$\alpha_p = \frac{\frac{N_c}{2p} - k_1}{\frac{N_c}{2p}} + k_2 = \frac{9-1}{9} + 0,02 = 0.9089$$

$$\Rightarrow BetaM = 0.9089 \cdot 180°\text{el} = 163.6°\text{el}. \qquad (3)$$

3.3 Optimization process

In order to run the optimization it is necessary to link Matlab, SPEED and MotorCAD into a logical system as shown in Fig. 7. The linkage is done via ActiveX. The

Matlab handles the communication between programs and runs the optimization algorithm. The SPEED software receives the parameters from Matlab that are optimized, performs the electromagnetic calculation and returns the results to Matlab. The MotorCAD performs thermal calculation according to the SPEED model and returns the results to Matlab. The results from SPEED and MotorCAD are used to evaluate the constraint functions in the optimization process.

Fig. 8 shows the cross-section of the 18/16 model with parameters that are being optimized. Those parameters are: stator outer diameter D_o, magnet thickness h_m, stator bore diameter D, stator slot depth SD, stator tooth thickness TWS, thickness of the stator tooth tip TGD, width of the stator slot opening SO, shaft radius $RadSH$, stack axial length L_{stk}, slot opening angle S_{oang} and maximum current density J. The actual variables used in the DE algorithm are not necessarily the numerical values of those parameters in their actual units. It is much more efficient if most of the parameters are normalized with respect to some other values. For instance, it is always better to define the ratio of the tooth thickness TWS and the slot pitch τ_s as a variable instead of the actual value of the tooth thickness because, depending on the diameter of the stator bore, the actual tooth thickness that emerges from the DE algorithm after mutation might be greater than the slot pitch which leads to geometrically unfeasible solution and the generation of error message from the SPEED software. However, if the normalized tooth thickness with respect to the slot pitch is defined in the interval between 0.3 and 0.7, it will never yield an unfeasible geometry of the motor. Table 3 shows the actual normalized variables for the 18/16 model that are being optimized and their boundary constraints. For the 12/10 model the lower boundary for D_o/D_{omax} is 0.5 and the lower boundary for L_{stk}/D_{omax} is 0.2, while the remaining parameters are the same for both models.

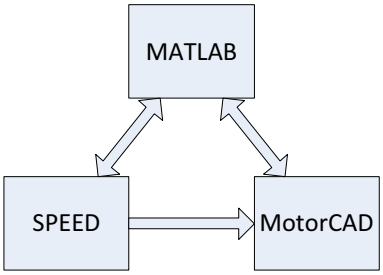

Fig. 7. Matlab–SPEED–MotorCAD logical linkage diagram

The value of D_{omax} is 200 mm for the 12/10 model and 250 mm for the 18/16 model. Due to higher number of poles in the case of 18/16 model, a larger stator outer diameter was expected. However, the optimization yielded

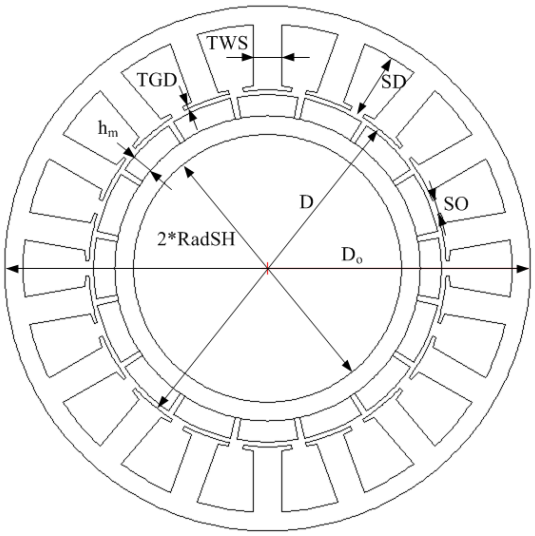

Fig. 8. Cross-section of 18/16 model with parameters that are optimized

Table 3. Parameters for the 18/16 model that are being optimized and their boundary constraints

Parameter (relative)	**Boundaries**
D_o/D_{omax}	[0.4, 1]
L_{stk}/D_{vmax}	[0.1, 1]
h_m/δ	[2, 6]
D/D_o	[0.4, 0.8]
$SD/\frac{D_o-D}{2}$	[0.4, 0.9]
TWS/τ_s	[0.3, 0.7]
TGD/SD	[0.05, 0.2]
S_{oang}, degrees	[1, 30]
$SO/(\tau_s - TWS)$	[0.1, 0.9]
J, A/mm^2	[4, 22]
$RadSH/\frac{D-2\delta}{2}$	[0.4, 0.9]

a smaller diameter for 16 poles than in the case of 10 poles. The control parameters of the DE algorithm are set to $F = 0.5$, $CR = 0.8$, strategy=DE/best/1/exp. The population size is $NP = 120$.

3.3.1 Constraints

The results from SPEED and MotorCAD are used to calculate the constraints in the optimization process. The constraints are not embedded in the cost function using penalty parameters or weights. Instead, an algorithm proposed by Lampinen [13] has been used. The motor must

meet the following constraints:

1. Stator tooth flux density lower than 2 T,
2. Stator yoke flux density lower than 1.5 T,
3. Rotor yoke flux density lower than 1.5 T,
4. Shaft power greater than or equal to 15 kW,
5. Maximum winding temperature lower than 155 °C (limit of class F insulation),
6. Mass of active parts lower than 50 kg (this condition has been placed tentatively since by minimizing the volume, which is the cost function, the mass is also minimized).

The stator tooth flux density, stator yoke flux density, rotor yoke flux density, shaft power and maximum mass are taken from the results of the SPEED dynamic simulation, while the maximum temperature is taken from the results of the MotorCAD static simulation. It is assumed that class H insulation is used for the winding, but the maximum allowed temperature is within limits of the class F insulation.

3.3.2 Cost function

The cost function F_c whose value is being minimized is equal to the difference of the volumes of two cylinders, one limited by the outer diameter of the stator core D_o and the stack length L_{stk}, and the other limited by the shaft diameter ($2 \cdot RadSH$) and the stack length. This can be written in the form

$$F_c = \frac{\pi}{4}\left[D_o^2 - (2RadSH)^2\right] L_{stk}. \tag{4}$$

3.3.3 Calculation of the control current

The SPEED software requires the peak value of the sinusoidal reference current waveform (parameter ISP) that the current controller can provide to be defined. The value of ISP is calculated within a Matlab function by multiplying the optimization parameter J that represents the absolute maximum current density with the surface of the copper in the slot divided by the total number of turns in the slot. The number of turns per coil is defined using the parameter TC in SPEED. Since two-layer winding is used, the parameter TC is multiplied by two to get the total number of turns in the slot. The slot area is available as the output parameter $Aslot$ from SPEED, so the copper area in the slot is obtained by multiplying the slot area with 0.4, which is the common slot fill factor in the case of round copper wire.

3.3.4 Calculation of the number of turns per coil

The slot area $Aslot$ and the slot fill factor SFg determine the total ampereturns in the slot. However, one must determine the number of turns per coil TC which in turn defines the value of the parameter ISP, because $Aslot \cdot SFg = 2 \cdot TC \cdot ISP$. The parameter TC must be varied to obtain the maximum torque in the motor mode, because it directly affects the value of the back EMF. This is done through the program loop in the Matlab function which calculates the torque for every TC (integer value), starting from the value 1, and stores the number of turns for the maximum torque. The loop runs until TC, i.e. the back EMF, is high enough so that the generator mode is achieved when torque becomes negative. In that case the execution of the loop breaks and the stored value of the number of turns corresponding to the maximum torque is entered in SPEED as the value of TC.

3.4 Optimization results

The results refer to the ambient temperature 20 °C, because the motor will work in such conditions at altitudes higher than 1000 m. The motor is designed with forced cooling and the air speed of 15 m/s blowing axially across the frame, because the ultra light aircraft (glider) moves through the air with a minimum speed of 15 m/s, while the average speed is over 20 m/s. It is important to monitor the magnet temperature, especially during short-term overload, because the maximum operating temperature for the selected magnets is 180 °C and above that temperature the magnets lose their properties, i.e. they demagnetize. The magnet properties used in the simulations are: manufacturer SINOMAG, grade N38UH, remanence at 20°C $B_r = 1.237$ T , coercivity at 20°C $H_c = -964$ kA/m, temperature coefficients of remanence and coercivity $CB_r = -0.11\%/°\text{C}$, $CH_c = -0.60\%°\text{C}$.

Table 4. Optimization results for the BLDC motor with 12 slots and 10 poles after 132 iterations

Best=1178685, F=0.5, CR=0.8, NP=120	
D_o/D_{omax}	0.5948
L_{stk}/D_{omax}	0.6707
h_m/δ	4.1367
D/D_o	0.6428
$SD/\frac{D_o-D}{2}$	0.7110
TWS/τ_s	0.4785
TGD/SD	0.0527
S_{oang}	6.2138°
$SO/(\tau_s - TWS)$	0.1517
J	19.4674 A/mm^2
$RadSH/\frac{D-2\delta}{2}$	0.7311

Table 5. Optimization results for the BLDC motor with 18 slots and 16 poles after 166 iterations

Best=864715, F=0.5, CR=0.8, NP=120	
D_o/D_{omax}	0.4448
L_{stk}/D_{omax}	0.4808
h_m/δ	4.4711
D/D_o	0.6790
$SD/\frac{D_o-D}{2}$	0.7793
TWS/τ_s	0.4623
TGD/SD	0.0545
S_{oang}	3.4174°
$SO/(\tau_s - TWS)$	0.4456
J	21.7486 A/mm^2
$RadSH/\frac{D-2\delta}{2}$	0.7705

Table 4 shows the optimization results for the 12/10 motor and Table 5 shows the optimization results for the 18/16 motor. *Best* is the motor active part volume (value of the cost function) in mm^3, *F* and *CR* are the DE control parameters, and *NP* is the population size. The optimal values of *F* and *CR* are dependent on both the objective function characteristics and the population size.

Depending on the weather conditions, the pilot of the aircraft might sometimes require extra power from the motor beyond its rated 15 kW. The maximum power capability depends on the available DC bus voltage, the motor back EMF and the winding resistances and inductances. Table 6 shows the features of both motors in a variety of working conditions and the results indicate that the maximum available power for the 12/10 motor is 37 % above its rating. If the motor is started from the cold state, it can endure this load for 95 to 120 seconds before reaching the maximum allowed temperature of 155 °C, depending on the ambient temperature. For the 18/16 motor the maximum power is 84 % beyond its rating which can last for 30 to 37 second. Of course, the actual duration of the operation at maximum power depends on the winding temperature prior to applying the overload, which may be higher than the ambient temperature if the aircraft is already flying and using the motor for propulsion. Based on experience with measured and calculated thermal transients of the SPM motor shown earlier in the paper, one must take the results in Table 6 with caution when using the deafult thermal model from MotorCAD. Table 7 shows fundamental components of current and back-emf and their relationship to the electromagnetic power. The shaft power is obtained by subtracting the core losses, and the windage and friction losses from the electromagnetic power.

4 CONCLUSION

The combined implementation of the SPEED and MotorCAD software, Differential evolution optimization algorithm and Matlab for the purpose of finding an optimized design of a brushless DC motor for the propulsion of an ultra light aircraft has been presented.

Two brushless DC permanent magnet motors have been designed, one with a combination of slots and poles 12/10, and the other with a combination of slots and poles 18/16. The purpose of increasing the number of poles after obtaining the optimal 12/10 design was to yield further reduction in mass and volume, since the machine with larger number of poles has a higher torque density. The further increase of the number of slots and poles beyond 18/16 is not possible due to limitation of the outer diameter of the motor since the space available on the aircraft is also limited. With larger number of poles within fixed dimensions it would not be possible to accommodate higher number of slots in the motor without running into problems with magnetic saturation of the stator teeth.

The motor with 18 slots and 16 poles proved to be a better solution for aviation purposes because it meets the requirements of the project (small mass and volume) better than the 12/10 motor. It also has a more trapezoidal back-EMF waveform and has a higher overload capacity, which is very important in the case of unfavorable weather conditions during the flight. In addition, the combination of slots and poles 18/16 effectively eliminates cogging torque, so the skew of the stator slots is not necessary and the motor is cheaper.

Due to the time limit and the long duration (40-45 hours) of the optimization process, only one strategy for Differential evolution algorithm has been tested and the DE control parameters (F and CR) have been changed only once. It may be possible to find a better solution with optimal parameters F and CR, but they are difficult to determine. The selected optimization strategy (DE/best/1/exp) is a good choice for technical problems, but there is a possibility of finding a better solution by using other strategies and the corresponding parameters F and CR.

APPENDIX A COMPARISON OF FINAL RESULTS

Figures 9 to 15 show comparison between the motor with 12 slots and 10 poles and the motor with 18 slots and 16 poles in terms of current, back EMF, cogging torque, total electromagnetic and shaft torque, and overload capacity. The figures indicate that the motor with 18 slots and 16 poles is a better solution and therefore will be selected for prototype development.

Table 6. Motor 1 (12/10) / Motor 2 (18/16) features in different working conditions

Shaft power, W		**RMS Current, A**		**Ambient temperature,°C**	**Maximum temperature, °C**		**Magnet temperature, °C**		**Working time, s**	
12/10	*18/16*	*12/10*	*18/16*		*12/10*	*18/16*	*12/10*	*18/16*	*12/10*	*18/16*
14927	14950	194.0	211.1	20	154.6	155.9	60.9	81.8	∞	∞
13538	13338	175.7	189.0	40	153.3	154.9	76.4	95.6	∞	∞
20500	27600	275.6	409.5	20	278.5	462.7	22.2	21.1	120	37
20500	27600	275.6	409.5	40	299.5	485.1	41.6	40.8	95	30

Table 7. Fundamental components of current and back-emf and their relationship to electromagnetic power

Fundamental phase back-emf $E_{1_{rms}}$, V		**Fundamental phase current $I_{1_{rms}}$, A**		**cosφ**		**Electromagnetic Power $P_{em} = 3E_{1_{rms}}I_{1_{rms}}cos\varphi$, W**		**Shaft Power, W**	
12/10	*18/16*	*12/10*	*18/16*	*12/10*	*18/16*	*12/10*	*18/16*	*12/10*	*18/16*
35.0	30.6	190.3	206.3	0.763	0.815	15235	15417	14927	14950
33.7	29.5	172.0	183.8	0.797	0.849	13850	13799	13538	13338
42.2	43.3	274.1	408.1	0.604	0.533	20930	28224	20500	27600

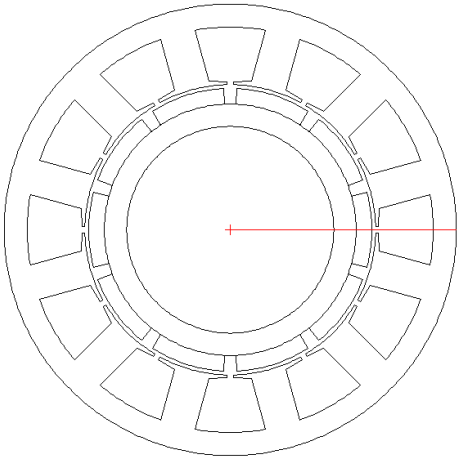

(a) 12/10

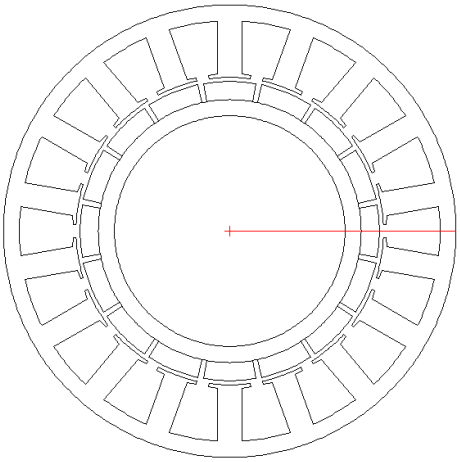

(b) 18/16

Fig. 9. Cross-sections of both motors in SPEED

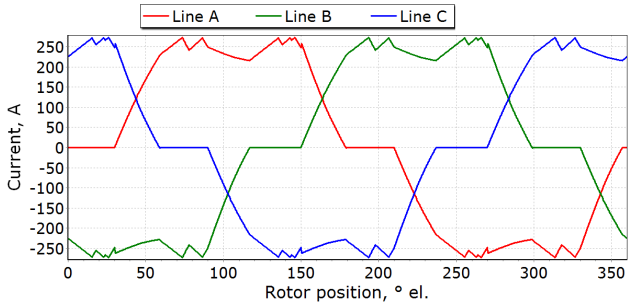

(a) 12/10

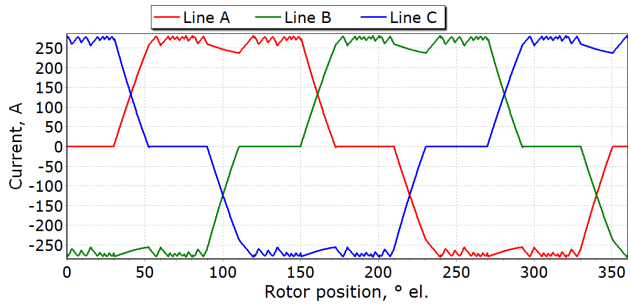

(b) 18/16

Fig. 10. Current waveforms of both motors in SPEED

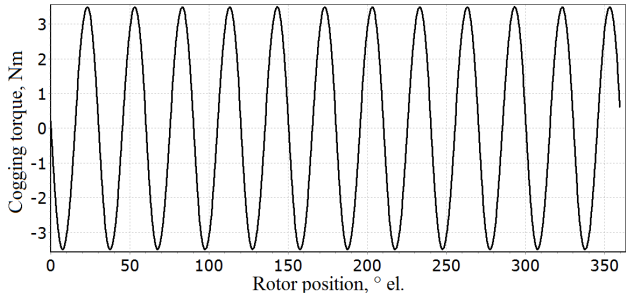

(a) 12/10

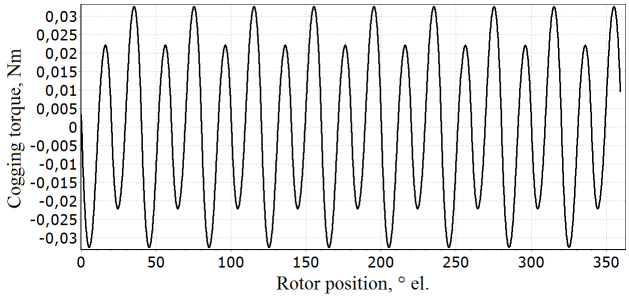

(b) 18/16

Fig. 13. Cogging torque waveforms of both motors in SPEED without stator slot skew

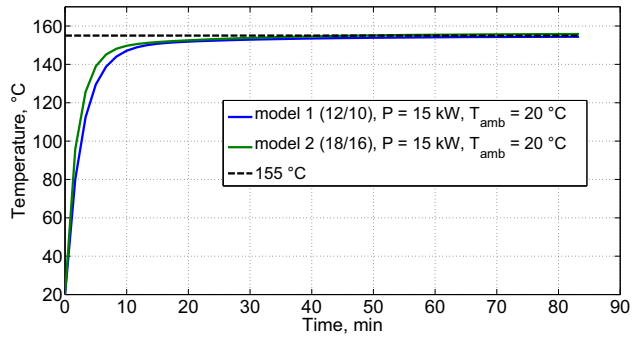

Fig. 14. MotorCAD thermal transients for continuous operation at rated power and ambient temperature 20 °C

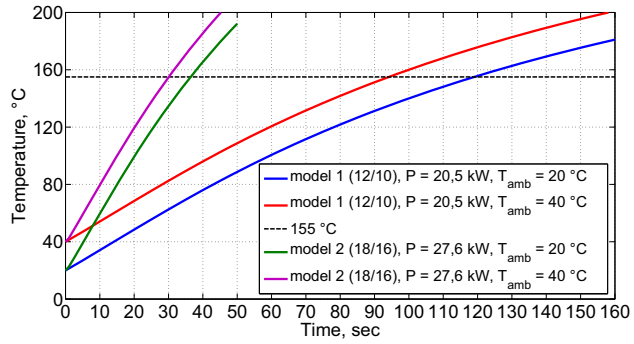

Fig. 15. MotorCAD thermal transients for operation at maximum power and ambient temperatures 20 °C and 40 °C

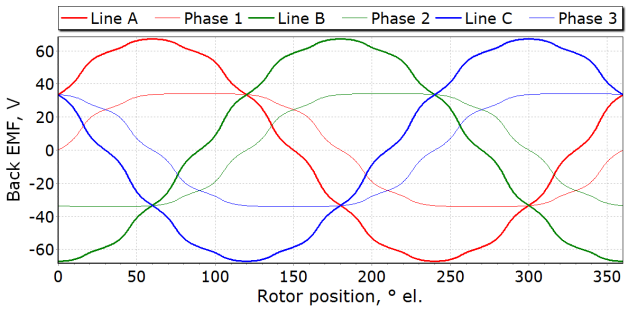

(a) 12/10

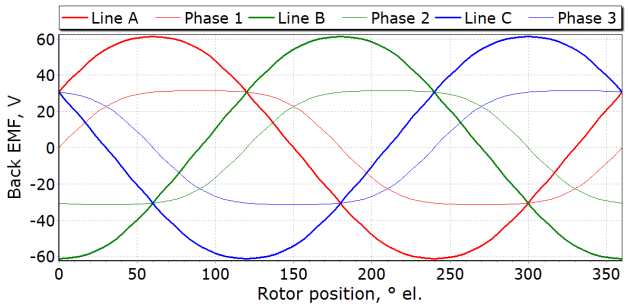

(b) 18/16

Fig. 11. Back EMF waveforms of both motors in SPEED

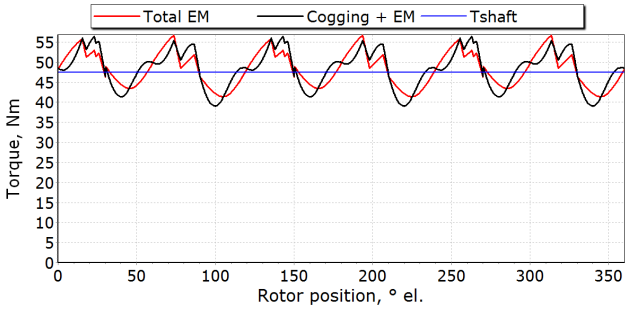

(a) 12/10

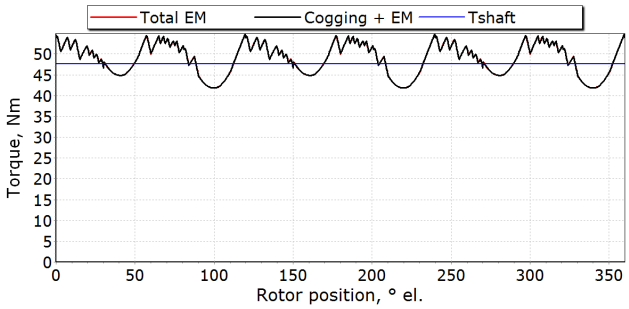

(b) 18/16

Fig. 12. Torque waveforms of both motors in SPEED

REFERENCES

[1] R. M. Crowder, *Electric drives and their controls*. Oxford: Clarendon Press, 1995.

[2] P. Ragot, M. Markovic, and Y. Perriard, "Optimization of Electric Motor for a Solar Airplane Application," *IEEE Trans. Ind. Electron.*, vol. 42, pp. 1053–1061, July/August 2006.

[3] Y. Perriard, P. Ragot, and M. Markovic, "Brushless DC Motor Optimization Process - Choice between Standard or Straight Tooth Shape," in *Conference Record of the 2006 IEEE Industry Applications Conference Forty-First IAS Annual Meeting*, pp. 1898–1904, 8-12 Oct. 2006.

[4] P. Ragot, P. Germano, M. Markovic and Y. Perriard, "Brushless DC motor for a solar airplane application: comparison between simulations and measurements," in *2008 IEEE Industry Applications Society Annual Meeting*, pp. 1–6, 5–9 Oct. 2008.

[5] R.J. Hill-Cottingham, P.C. Coles, J.F. Eastham, F. Profumo, A. Tenconi, and G. Gianolio, "Multi-disc axial flux Stratospheric Aircraft Propeller Drive," in *Conference Record of the 2001 Ieee Industry Applications Conference Thirty-sixth IAS Annual Meeting*, pp. 1634–1639, 30 Sep.–4 Oct. 2001.

[6] P.J. Masson, D.S. Soban, E. Upton, J.E. Pienkos, and C.A. Luongo, "HTS Motors in Aircraft Propulsion: Design Considerations," *IEEE Trans. Appl. Supercond.*, vol. 15, pp. 2218–2221, June 2005.

[7] P.J. Masson, and C.A. Luongo, "High Power Density Superconducting Motor for All-Electric Aircraft Propulsion," *IEEE Trans. Appl. Supercond.*, vol. 15, pp. 2226–2229, June 2005.

[8] P.J. Masson, J.E. Pienkos, and C.A. Luongo, "Scaling Up of HTS Motor Based on Trapped Flux and Flux Concentration for Large Aircraft Propulsion," *IEEE Trans. Appl. Supercond.*, vol. 17, pp. 1579–1582, June 2007.

[9] P.J. Masson, M. Breschi, P. Tixador, and C.A. Luongo, "Design of HTS Axial Flux Motor for Aircraft Propulsion," *IEEE Trans. Appl. Supercond.*, vol. 17, pp. 1533–1536, June 2007.

[10] A. M. EL-Refaie, "Fractional-Slot Concentrated-Windings Synchronous Permanent Magnet Machines: Opportunities and Challenges," *IEEE Trans. Ind. Electron.*, vol. 57, pp. 107–121, January 2010.

[11] D. Ishak, Z.Q. Zhu and D. Howe, "Comparison of PM Brushless Motors, Having Either All Teeeth or Alternate Teeth Wound," *IEEE Trans. Energy Convers.*, vol. 21, no. 1, 2006.

[12] Z.Q. Zhu and D. Howe, "Influence of Design Parameters on Cogging Torque in Permanent Magnet Machines," *IEEE Trans. Energy Convers.*, vol. 15, no. 4, 2000.

[13] J. Lampinen, "Multi-Constrained Nonlinear Optimization by the Differential Evolution Algorithm," *6th On-line World Conference on Soft Computing in Industrial Applications (WSC6)*, September 10–24 2001.

Mario Jurković received the M.Sc. degree in electrical engineering from the University of Zagreb, Faculty of Electrical Engineering and Computing, Croatia in 2011. Currently he is a design engineer in KONCAR Distribution and Special Transformers, Inc. where he works on design of distribution and special transformers (oil immersed and dry type) and shunt reactors. His research interests are in design and optimization of electrical machines. He received the "Josip Lončar" student award for academic excellence from the Faculty of Electrical Engineering and Computing and the "INETEC" student award from the Institute for Nuclear Technology, Zagreb, Croatia.

Damir Žarko received the B.Sc. and M.Sc. degrees in electrical engineering from the University of Zagreb, Faculty of Electrical Engineering and Computing, Croatia in 1995 and 1999 respectively and the Ph.D. degree from the University of Wisconsin-Madison, USA in 2004. Currently he is an Associate Professor at the University of Zagreb, Faculty of Electrical Engineering and Computing, Department of Electrical Machines, Drives and Automation. He teaches undergraduate and graduate level courses on design and theory of electrical machines and transformers. His research activities are related to design, modelling, analysis and optimization of electrical machines and drives. He is a member of IEEE and the Croatian National Committee of CIGRÉ.

AUTHORS' ADDRESSES

Mario Jurković, M.Sc.
KONCAR Distribution and Special Transformers, Inc.
Mokrovićeva 8, P.O.Box 100 HR-10090 Zagreb, Croatia
email: mario.jurkovic117@gmail.com

Prof. Damir Žarko, Ph.D.
University of Zagreb
Faculty of Electrical Engineering and Computing
Unska 3, 10000 Zagreb, Croatia
email: damir.zarko@fer.hr

Received: 2011-09-28
Accepted: 2012-04-02